

Article citation info:

Adamkiewicz A, Nikończuk P. An attempt at applying machine learning in diagnosing marine ship engine turbochargers. *Eksploracja i Niezawodność – Maintenance and Reliability* 2022; 24 (4): 795–804, <http://doi.org/10.17531/ein.2022.4.19>

## An attempt at applying machine learning in diagnosing marine ship engine turbochargers

Indexed by:



Andrzej Adamkiewicz<sup>a</sup>, Piotr Nikończuk<sup>b</sup>

<sup>a</sup>Maritime University of Szczecin, Faculty of Mechanical Engineering, ul. Wały Chrobrego 1-2, 70-500 Szczecin, Poland

<sup>b</sup>West Pomeranian University of Technology, Faculty of Maritime Technology and Transport, al. Piastów 17, 70-310 Szczecin, Poland

### Highlights

- Machine learning simplified the decision to renew the turbocharging system of the marine engine.
- The set of controlled parameters was minimized for the needs of diagnostic relationships.
- Ease of making maintenance decisions based on the maintenance requirement index.
- The results were verified with experimental data from engine tests of two types of turbochargers.

### Abstract

The article presents a diagnosis of turbochargers in the supercharging systems of marine engines in terms of maintenance decisions. The efficiency of turbocharger rotating machines was defined. The operating parameters of turbocharging systems used to monitor the correct operation and diagnose turbochargers were identified. A parametric diagnostic test was performed. Relationships between parameters for use in machine learning were selected. Their credibility was confirmed by the results of the parametric test of the turbocharger system and the main engine, verified by the coefficient of determination. A particularly good fit of the describing functions was confirmed. As determinants of the technical condition of a turbocharger, the relationship between the rotational speed of the engine shaft, the turbocharger rotor assembly and the charging air pressure was assumed. In the process of machine learning, relationships were created between the rotational speed of the engine shaft and the boost pressure, and the indicator of the need for maintenance. The accuracy of the maintenance decisions was confirmed by trends in changes in the efficiency of compressors.

### Keywords

This is an open access article under the CC BY license (<https://creativecommons.org/licenses/by/4.0/>)

machine learning, compressor diagnosis, marine ship engine, operational decision, neural network.

## 1. Introduction

Diesel engines dominate in 95% of the main propulsion of modern cargo sea vessels. As a result of normal wear and tear, as well as random interactions, they are subject to evolutionary degradation of their technical condition. Effective engine operation requires a reliable identification of the causes of wear of its systems and components, especially accelerated wear, of varying degrees of importance. Important systems, the failure or damage of which poses a threat to the performance of the transport task by the ship, include: the piston-cylinder system, the crank system and the turbocharging system, which, according to [31], causes 24.7% of all engine damage.

The analysis of the impact of the degradation of the technical condition of the turbocharging system components on the operating parameters, economy and reliability of marine engines was carried out in [4] with the use of the Kongsberg turbocharged marine engine simulator. The reliability analysis of such a system was performed in [3]. The reliability model of a ship engine cooperating with a turbocharger was considered in [22], using the Weibull distribution for this purpose. The need to recognize the real effects of limiting the ef-

iciency of rotating machinery and possible failure of the turbocharger in the turbocharging system of the marine engine was obtained based on the results of simulation tests described in [11]. The ecological consequences of the operation of a malfunctioning two-stroke engine turbocharger regarding NOx emissions are included in the complete analysis presented in the paper [13]. The publication [30] presents the results of an extended plan of experiments on a turbocharged four-stroke marine engine. By modifying the engine air intake manifold for additional compressed air supply, it was possible to increase the air pressure downstream of the turbocharger compressor, thereby generating unstable operation. The measurement results were used to determine the range of the unstable operation field on the compressor characteristics and the form of instability at any point in the engine operating field. The paper [20] presents a mathematical model constituting the basis of a simulation model of steady and transient operation of a turbocharged, slow-speed compression-ignition engine. Particular attention was paid to the study of the stability and measurement availability in difficult conditions, such as difficulties in cleaning the interscapular channels. In the work [28], a systematic analysis of friction losses in the turbocharger bearings was carried out.

(\*) Corresponding author.

E-mail addresses: A. Adamkiewicz (ORCID: 0000-0002-8314-0660): [a.adamkiewicz@pm.szczecin.pl](mailto:a.adamkiewicz@pm.szczecin.pl), P. Nikończuk (ORCID: 0000-0002-7809-7653): [piotr.nikonczuk@zut.edu.pl](mailto:piotr.nikonczuk@zut.edu.pl)

Figure 1 shows the contaminated rotor of the ABB TPL 67-C type 6L50 DFDE turbocharger radial compressor, with salt deposits on the rotor blades emphasizing the contours of the impressions of the disassembled diffuser blades around the rotor (photo a) and a view of the rim of contaminated turbine expansion devices, after exceeding the resource working hours of the turbocharger by over 2000 (photo b) of the turbine powered by marine fuel combustion products.

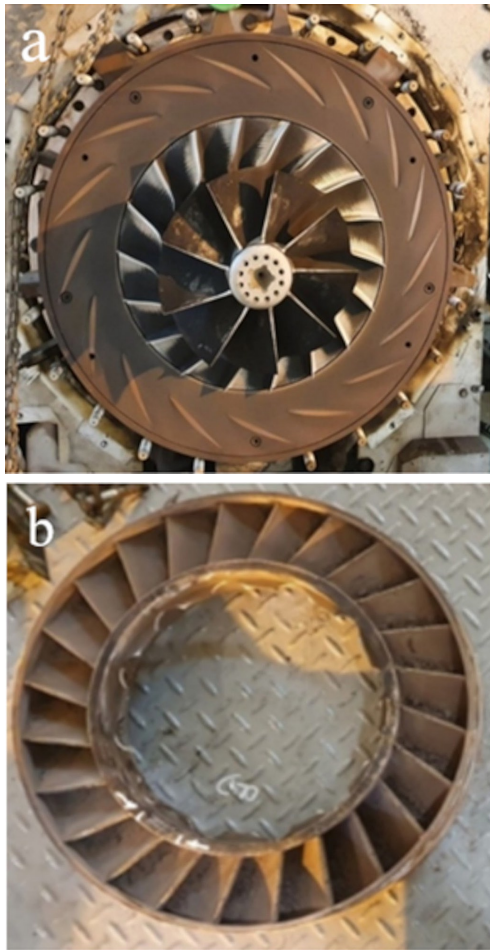


Fig. 1. View of flow canals of a rotor in a radial compressor (a) with blades of turbine expansion instruments (b) of the ABB TPL 67-C type compressor contaminated during a normal operation of a marine engine turbocharging system

The channels between the compressor blades are covered with contaminants contained in the aspirated sea spray and oil vapours passing through the seals between the compressor rotor and the bearings. Hard deposits of sea salt mixed with components of exhaust fumes and industrial dust in coastal areas change the surface condition of the flow channels, the geometry of the blades and, consequently, the characteristics of the machines. By increasing the imbalance of the rotor assembly, the deterioration of the technical condition of the rotor blades contributes to an increase in rotor mass and vibration of the rotor shaft and accelerates bearing wear. The likelihood of pumping increases, which precludes further operation of the turbocharging system. Figure 2 shows the view of the rim blades of the turbine expansion devices of the ABB TPL 67-C turbine with discoloration of tar deposits, carbon deposits from incomplete and incomplete fuel combustion and oil vapours from leaks in the lubrication system. The confrontation of the examples of the surface condition of the blades of the expansion

devices shown in Figures 1b and 2 confirms the possibility of large differences in the properties of the deposits on the blades at various stages of operation, their random thicknesses and distributions determining the quality and nature of energy conversion processes in the channels between the turbine blades, and consequently the efficiency of compressors and turbines.



Fig. 2. Blade rim of expansion instruments of a turbocharger of the ABB TPL 67-C type contaminated with deposits of fuel combustion products

Experimental studies for the real 3AL25 / 30 four-stroke marine engine are presented in [31]. Based on the results of an active experiment on a technical scale, the share of contaminants and sediments of individual elements of the turbocharging system in the impact on the engine operating parameters was given, as shown in Figure 3. Contamination concerns the compressor flow channels in 56%, the turbine flow channels 22%, the air cooler 11%, air filters 6%, compressor and turbine rotor channel cleaning systems 4%, other elements 1%.

In practice, the number of measured parameters of the turbocharging system operation does not provide sufficient information about the quality of energy conversion processes to determine the efficiency of rotating machines, and, consequently, about the need to perform services that reconstruct the technical condition of the inter-vane rotating machines channels. The technical condition of the surface of the blades has a direct impact on the efficiency of the compressor and turbine. However, to determine them, it is necessary to know the operating parameters measured during the operation of the engine and turbocharger.

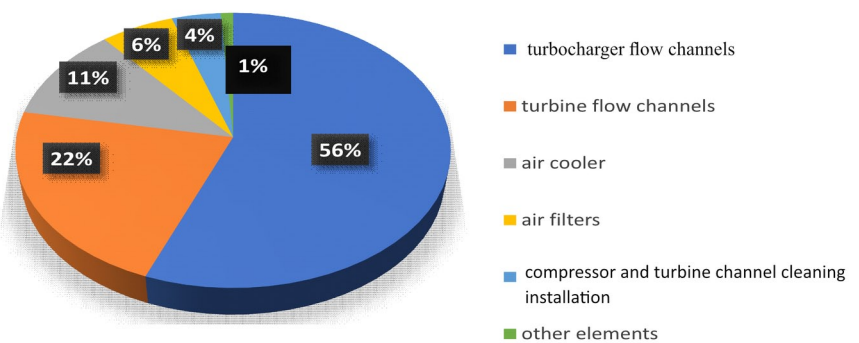


Fig. 3. Contribution of contaminants and sludge to the effect on engine performance

The article [6] presents the concept of diagnosing the exhaust tract for monitoring the state of the turbocharger of the ship's main engine. The flue gas flow rate indicator was proposed, characterizing the flue gas volume flow and isentropic efficiency, as two dimensionless

indicators for assessing the technical condition of the turbocharger. Moreover, the non-linear relationship between these two indicators and the measurable parameters of the exhaust tract of the turbocharger was investigated. A novel method for assessing the degradation of turbocharger efficiency has been defined. The paper [17] presents the influence of the surface roughness of the blades on the compressor efficiency and noise emission in the turbocharger of the diesel engine, while the paper [18] presents the results of numerical processing of the results of the acoustic signal parameters measurements in the turbocharger. The turbocharger condition monitoring system, especially for passenger vehicles, is presented in [14]. Possible malfunctions of turbochargers with their cause-effect relationships and frequency of occurrence were investigated. Compressor degradation (due to contamination with oil deposits and combustion product deposits, for example) was identified as the only malfunction worthy of further investigation. An approximate model of compressor efficiency reduction because of tar contamination of the blades was proposed by means of a regression function related to the actual, clean, and degraded compressor characteristics data. Based on the results of the simulation of a diesel engine based on an approximate model, it was found that when the efficiency of the compressor is reduced, three symptoms appear: increased blade angle adjustment in the turbine with variable geometry blades, which leads to an increase in the rotational speed of the rotor and an increase in air temperature at the outlet from the compressor. Limited diagnostics of malfunctions and prediction of turbocharger failures by means of the analysis of the thrust load of the turbocharger thrust bearing are presented in [33].

The methods and diagnostic models described above are based on large groups of measurement or simulation data. Neither of these methods is a solution to a diagnostic task based on a limited set of measured engine and turbo performance parameters. There is no method of assessing the efficiency of the rotating machinery of a turbocharger, necessary to assess the quality of energy conversion in a ship engine, and, consequently, to undertake maintenance activities, or replace components with new ones.

Attempts to use determined diagnostic models in the operational verification diagnostics of turbochargers encounter difficulties due to the limited availability of measurement of air and exhaust gas parameters in the turbocharging system and difficult-to-measure disturbances from accompanying processes.

In technical issues where there is no data to solve the problem based on known physical dependencies, energy conservation equations, artificial intelligence methods are often used. These methods do not operate with differential equations but are usually optimized dependency rules in the case of fuzzy logic or for neural networks a black box with weight connections between neurons with specific activation functions. Creating neural networks and learning their dependencies to obtain decision information is also called machine learning.

For the diagnosis of turbochargers, many methods and algorithms are proposed, extending the possibilities of using motor diagnostics [32]. There are known applications of fuzzy logic to control a turbocharger [10] as well as the identification of turbocharger operating parameters based on vibroacoustic signals [29] and the analysis of the vibration spectrum to identify damages [7]. There are also proposals to use neural networks to identify faults based on vibroacoustic signals from compressors [8] and piston internal combustion engines [25]. Machine learning has also been proposed to predict both damage to compressor blades [26] as well as compressor shutdown times [12]. The topic of prediction was also discussed in connection with forecasting operating parameters and potential inefficiencies of turbines [23] and predicting maintenance / servicing of turbochargers [16]. Predicting the need to repair car compressors using the service records and registered vehicle data is presented in [24]. The methods and results of the application of supervised machine learning techniques to the task of predicting the need for repair of air compressors in commercial trucks

and buses are described. The predictive models come from recorded on-board data collected during workshop visits. These data were collected over three years based on the performance of a large number of vehicles.

In the further part of the article, the authors present the concept of introducing the service necessity indicator  $M$ , which classifies a turbocharger for servicing. The value of the indicator is estimated based on the measured values of the engine speed and the boost air pressure from the turbocharger. An attempt was made to create a neural classifier to which known neural networks with feed-forward backpropagation were applied. For the computational work, measurement data from a marine engine operated in standard conditions were used, and a graphical interface for teaching *nnTool* neural networks in Matlab was used.

## 2. Problem formulation

Deterioration of compressor and turbine blade surfaces, changes the aerodynamics of the air and exhaust flow, reducing the flow capacity of the inter-blade canals of the rotating machines, which is reflected in [17]:

- change in the rotor unit speed;
- decrease of efficiency of turbocharger and engine machines;
- increase of engine fuel consumption,
- generation of vibrations resulting from the unbalance of the turbocharger rotor unit;

with simultaneous change of thermal and flow parameters of air and exhaust gases in the turbocharging system. The turbocharging system of the engine consists of a turbocharger with an air filter, noise silencer and charging air cooler. Fig. 4 shows a diagram of the system with marked control planes.

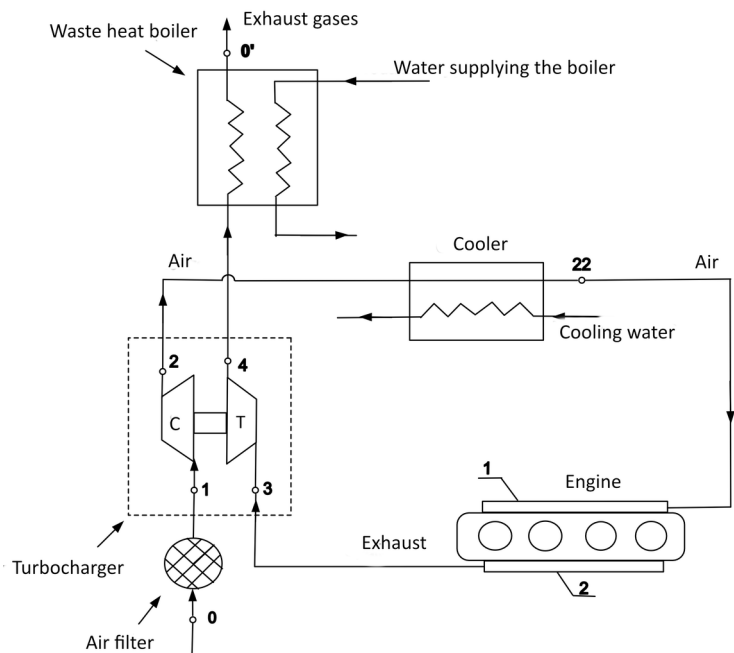


Fig. 4. Diagram of the turbocharging system for a marine diesel engine: 1 – charging air reservoir; 2 – exhaust gas collector

This paper studies a turbocharger consisting of a rotor unit mounted on bearings embedded in a hull with an exhaust gas collector. The rotor unit includes a radial compressor with straight blades and a rim of turbine blades, shafts connected by couplings, supported in bearing seats with thrust axial and sealing rings. A diagram of the turbocharger rotor unit with labelled control planes for the needs of a mathematical model is shown in Figure 5.

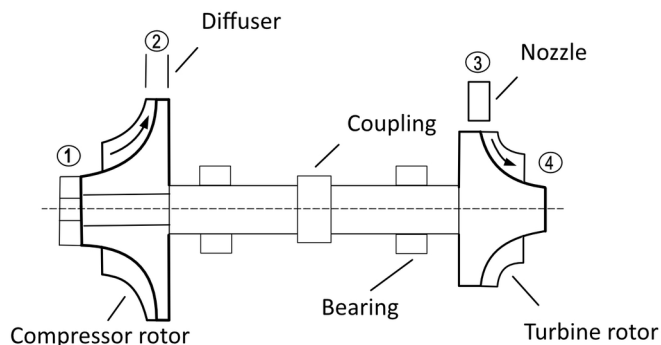


Fig. 5. Diagram of a turbocharger rotor unit with control plane numbers

Standard condition monitoring systems of turbocharging systems used on ships do not ensure the determination of compressor and turbine efficiency based on the results of current measurements of operational parameters. Not all necessary parameters of thermodynamic processes can be reliably accessed by measurements. If the key operational issue is to maintain the turbocharging system of the engine in the condition of the highest possible efficiency which does not decrease during its operation, it is necessary to control systematically the relationships between operational parameters in confrontation with admissible and limiting parameters. Operational parameters used for the evaluation of correctness of energy transformations in the turbocharger should serve as an argument for formulating service conclusions. However, the condition of task realization is the availability of operational parameters of the turbocharger subunits determining the methods of decision making or application of machine learning.

### 3. Efficiency of turbocharger rotating machines

In the mathematical model built, it was assumed that the measure of the quality of the air compression and exhaust gas expansion process is the isentropic efficiency of the compressor and turbine. The compression process was considered to be an adiabatic irreversible one with increasing entropy due to internal friction in the flow canals of the compressor. Figure 6 shows the air compression process in enthalpy-entropy coordinates, from the state of  $1^*(p^*1, t^*1)$  at the compressor inlet, to the state of  $2^*(p^*2, t^*2)$  at the compressor air outlet.

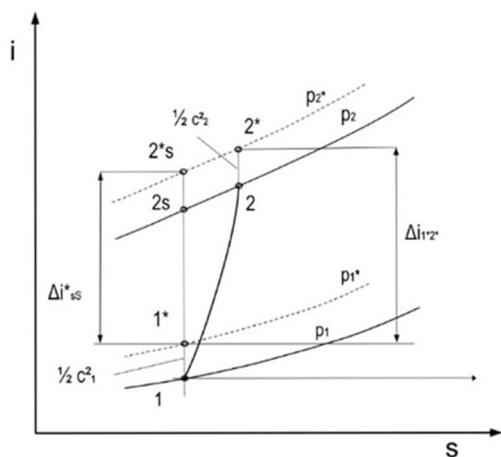


Fig. 6. The air compression process in enthalpy-entropy coordinates

According to the notational convention used in the model, the isentropic efficiency of the compressor  $\eta_c^*$  is defined as the ratio of the enthalpy gain of isentropic compression  $\Delta i_{sc}^*$  to the work of the actual compression  $l_c^* = \Delta i_{12}^*$

$$\eta_c^* = \frac{\Delta i_{sc}^*}{\Delta i_{12}^*} = \frac{\Delta i_{sc}^*}{l_{c12}^*} = \frac{i_{2s}^* - i_1^*}{i_2^* - i_1^*} \quad (1)$$

Treating air as semi-perfect gas and assuming for  $i^* = c_{pa}T^*$  the average specific heat of transformation  $c_{p12} = idem$  as constant, relation (1) will take the form of:

$$\eta_c^* = \frac{T_{2s}^* - T_1^*}{T_2^* - T_1^*} \quad (2)$$

The isentropic efficiency of compression in the total parameters between state  $1^*(p^*1, T^*1)$  and state  $2^*(p^*2, T^*2)$  considers the conversion of kinetic energy of the air in state  $2^*$  into static pressure energy, thus increasing in the outlet diffuser, the pressure of the charging air. By substituting the equation of the isentropic conversion into formula (2), the relation for the isentropic efficiency of compression expressed in the air state parameters determined by measuring the total pressures and temperatures at the air inlet and outlet from the compressor was obtained

$$\eta_c^* = \frac{\left(\frac{p_2^*}{p_1^*}\right)^{\frac{\kappa-1}{\kappa}} - 1}{\left(\frac{T_2^*}{T_1^*}\right) - 1} \quad (3)$$

where the properties of the air in transformation are described by the isentropic exponent for the air  $\kappa a = 1.4$ . The exhaust gas heat conversion process between the states  $3^*(p^*3, T^*3)$  and  $4^*(p^*4, T^*4)$  as the adiabatic transformation of the exhaust gas into the enthalpy-entropy coordinates is shown in Figure 7. Using the symbols shown in the graph (Fig. 7), the efficiency of the turbine  $\eta_T$  is defined as the ratio of the actual available enthalpy drop in the turbine  $\Delta i_{34}^*$  between states  $3^*(p^*3, T^*3)$  -  $4^*(p^*4, T^*4)$ , internal operation of the turbine  $l_{34}^*$ , to the isentropic available exhaust enthalpy drop  $\Delta i_{sT}^*$  between states  $3^* - 4_s^*$ .

$$\eta_T^* = \frac{\Delta i_{34}^*}{\Delta i_{sT}^*} = \frac{l_{34}^*}{\Delta i_{sT}^*} = \frac{i_3^* - i_4^*}{i_3^* - i_{4s}^*} \quad (4)$$

From the physics of conversion, the internal work of the turbine is smaller than the disposed isentropic enthalpy drop in the turbine due to frictional losses in real processes. Treating the exhaust gas as semi-perfect and assuming for  $i^* = c_{pg}T^*$  the average specific heat of transformation to be  $c_{p12} = idem$  the defining relationship (4) is formulated in the following form:

$$\eta_T^* = \frac{\Delta i_{34}^*}{\Delta i_{sT}^*} = \frac{T_3^* - T_4^*}{T_3^* - T_{4s}^*} \quad (5)$$

By substituting the isentropic equation into relation (5), we obtained the isentropic efficiency of the turbine expressed by measurable parameters of the state of exhaust gases before and after the turbine

$$\eta_T = \frac{1 - \left(\frac{T_4^*}{T_3^*}\right)}{1 - \left(\frac{p_4^*}{p_3^*}\right)^{\frac{\kappa-1}{\kappa}}}$$

where  $K_g = 1.33$  is the average isentropic exponent for marine fuel exhaust.

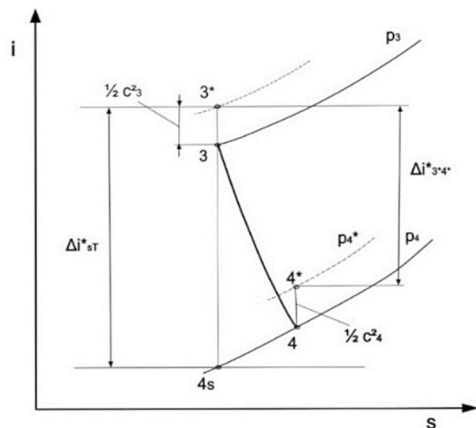


Fig. 7. Expansion process of exhaust gases in a single-stage turbine in enthalpy-entropy coordinates

Determination of compressor efficiency according to equation (3) and turbine efficiency according to relation (6) requires reliable measurements of air parameters in states 1 and 2 and exhaust parameters in states 3 and 4, in Figure 6.

Based on the experience of studies [31], [9], [15], [13] it was assumed that the informative character of operational diagnostics should ensure the assessment of the technical condition of a turbocharger based on values of observed operational parameters and enable to make important maintenance decisions based on a generalized parameter.

#### 4. Parametric diagnostic test

Cleaning of inter-blade channels of rotating machines belongs to the important and characteristic turbocharger services. The prerequisite for the identification of the sought-after malfunction is the knowledge of the relationships between the state characteristics and the parameters of the thermal-fluid signal and operational diagnostics]. Identification of relations, with simultaneous recognition of operational parameter measurement availability has been performed based on the population of marine engine turbochargers of several types.

To recognize measurability, variability, and relationships between the operational parameters of the turbocharging system, a passive operational experiment was carried out using a MAN type TCA55 turbocharger, cooperating with a Sulzer 6RTA48TB type main propulsion engine of 7 368 kW. The measurements were performed using standard control and measuring equipment [5]. Selected measurement results, in the form of courses of values of operational parameters of a turbocharger of the MAN TCA55 type: charging pressure  $p_2$  (Fig. 8), main engine rotational speed  $n_{ME}$ , turbocharger rotor speed  $n_{TC}$  (Fig. 9), air temperature in the engine room  $t_0$ , oil behind the turbocharger bearing  $t_{oil}$  and charging air behind the cooler  $t_{22}$  as a function of operation time (Fig. 10), represented by the numbers of consecutive observations, are shown in Figs. 8-10.

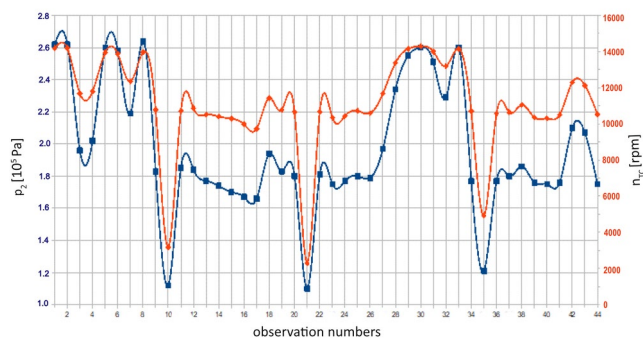


Fig. 8. Variability of charging pressure and turbocharger rotor speed as a function of observation numbers

The expected parameter of the charge exchange system is the charging air pressure  $p_2$ , whose strong relationships with the turbocharger rotor unit speed and engine shaft speed are shown by the runs in Figures 9 and 10.

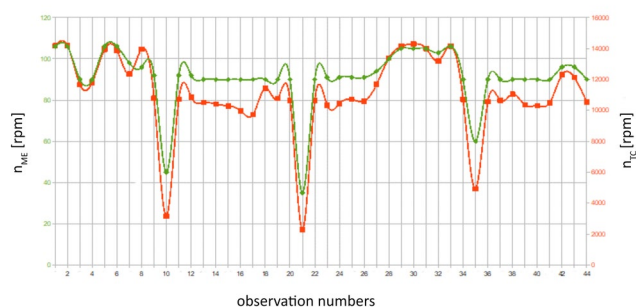


Fig. 9. The main engine speed and turbocharger rotor speed runs as a function of observation numbers

While the runs of the parameters in fig. 8 and 9 creating mutual relationships showed their diagnostic usefulness, the confrontation of the courses of air temperature in the engine room (temperature of sucked air at the beginning of compression), oil temperature behind the turbocharger bearing and charging air behind the cooler shown in fig. 10, are the parameters of different subunits and they do not show mutual relations.

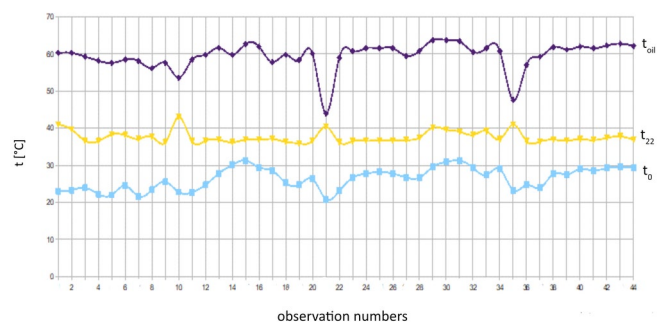


Fig. 10. Engine room air temperature, oil temperature behind the turbocharger bearing and charging air temperature after the cooler as a function of observation numbers

The value of air temperature behind the cooler is kept constant at  $t_{22} = 45.5^\circ\text{C} = idem$ . This temperature is regulated by a three-way valve in the LT (Low Temperature) cooling system, controlled by an air temperature sensor behind the cooler. Thus, the charging air temperature measured after the cooler is not a diagnostic parameter, it merely confirms correct functioning of the system.

During the period of the passive operational experiment, none of the monitored parameters of the turbocharger operation reached the limiting or admissible value. To evaluate the efficiency of the compressor based on formula (3) and turbine efficiency based on formula (6) it is necessary to know the measured air temperature directly behind the compressor  $T^*_2$  and the exhaust gas pressure before the turbine. In many types of turbochargers, as well as in the tested one, the manufacturers did not foresee the technical possibility to make this type of measurements.

Therefore, the operational experiment was extended to include measurements performed on turbocharging systems of four main engines of the MAK M43 type with a turbocharger of the ABB TPL 77 type, equipped with the possibility of measuring the air temperature behind the compressor  $t_2$  [2]. During one observation, the following were measured: air temperature at the turbocharger inlet  $t_1$ , air temperature  $t_2$  and air pressure  $p_2$  after the compressor, air temperature at the air cooler outlet  $t_{22}$ , exhaust gas temperature before the turbine  $t_3$

and after the turbine  $t_4$ , rotational speed of the turbocharger rotor unit  $n_{TC}$ , pressure drop at the air cooler  $\Delta p_{2,22}$ , and fuel delivery indicator at the fuel pump  $x$ . Measurement observations were made once a day and marked with consecutive numbers. The correctness of the measurements was verified by determining the quality measure of the model fit using the coefficient of determination  $R^2$ . Figure 11 presents graphically an example of air pressure after the compressors as a function of the turbocharger rotor speed of the four investigated engines [2]. The values of determination coefficients shown in the figure are in the range of 0.9-1.0, confirming their particularly good model fit and thus the diagnostic usefulness of the measured charging pressure.

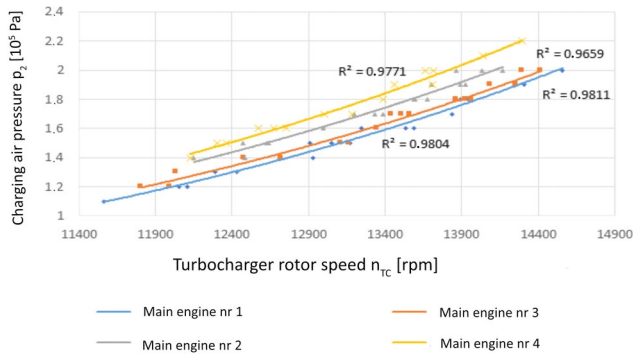


Fig. 11. Air pressure after compressor  $p_2$  versus rotor speed  $n_{TC}$  of ABB TPL 77 turbocharger

Using the results of measurements obtained during these observations, compressor efficiencies were calculated in accordance with equation (3) in various technical states of the surfaces of compressor inter-blade canals, before and after washing, before and after replac-

Table 1. Calculated compressor efficiencies

| Engine number / Observation number | nr 1 $\eta_c$ [%] | nr 2 $\eta_c$ [%] | nr 3 $\eta_c$ [%] | nr 4 $\eta_c$ [%] |
|------------------------------------|-------------------|-------------------|-------------------|-------------------|
| 1                                  | 38.53             | 47.70             | 51.53             | -                 |
| 2                                  | 27.45             | 36.64             | 43.93             | 76.59             |
| 3                                  | 29.15             | 33.70             | 41.73             | 43.62             |
| 4                                  | 23.88             | 33.79             | 41.62             | 42.69             |
| 5                                  | 31.03             | 41.84             | 44.52             | 44.74             |
| 6                                  | 14.32             | 17.61             | 34.94             | 40.68             |
| 7                                  | 44.15             | 52.27             | -                 | 51.17             |
| 8                                  | 20.69             | 30.42             | 29.79             | 36.50             |
| 9                                  | 14.48             | 24.84             | 30.98             | 30.24             |
| 10                                 | -                 | -                 | -                 | -                 |
| 11                                 | 43.89             | 53.41             | -                 | 53.37             |
| 12                                 | -                 | -                 | -                 | -                 |
| 13                                 | -                 | 47.85             | 49.21             | 53.27             |
| 14                                 | 34.89             | 44.20             | 46.85             | 47.52             |
| 15                                 | 33.33             | 41.94             | 48.43             | 47.97             |
| 16                                 | 20.31             | 28.94             | 33.79             | 36.26             |
| 17                                 | 39.61             | 50.12             | 40.22             | -                 |
| 18                                 | 31.24             | 40.85             | 45.07             | -                 |
| 19                                 | 8.33              | -                 | -                 | -                 |
| 20                                 | 26.51             | 16.56             | 47.40             | 39.24             |
| 21                                 | 42.56             | 37.19             | 53.15             | -                 |
| 22                                 | -                 | -                 | 40.69             | -                 |
| 23                                 | -                 | 49.73             | 46.33             | 54.75             |

ing the dirty air filter. The results of these calculations are presented in Table 1.

The obtained results of calculations for each of the engines, from the whole measurement series, have been confronted with the reference parameters of engine no. 1, presented in table 2 [1]. The compressor efficiency adopted the values fitting correctly into the ranges of reference parameters, consistent with the physics of wear and aging processes.

Table 2. Chosen reference parameters of the ABB TPL 77 type turbocharger engine

|  |       |       |       |       |
|--|-------|-------|-------|-------|
| Charging air press. $p_2$ [ $10^5$ Pa] | 1.074 | 2.394 | 2.943 | 3.302 |
| Load [%]                               | 50    | 85    | 100   | 110   |
| Engine Power $P_e$ [kW]                | 3900  | 6630  | 7800  | 8580  |
| Compressor efficiency [%]              | 6.02  | 50.80 | 57.10 | 59.24 |

Figure 12 shows trend patterns of decreasing compressor efficiency of the four engines at selected operating time intervals. They confirmed the nature of compressor efficiency changes and revealed differences in the rate of deterioration, when sailing in different hydrometeorological conditions. Only during short operation intervals, from 4 to 6 days (observation numbers), the tendency for cyclic decrease in efficiency and then its increase, after the compressor canal cleaning, turbine cleaning or air filter replacement, has been noted.

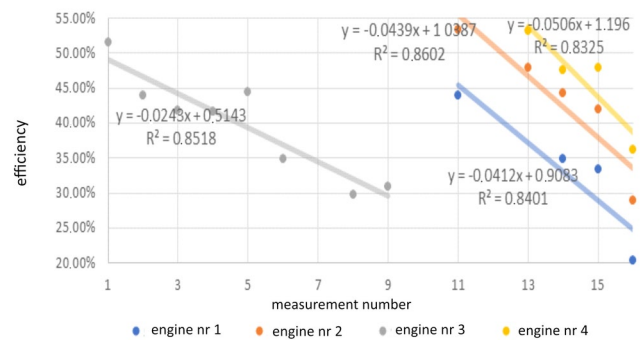


Fig. 12. Trends in compressor efficiency reduction for four engines in selected operational periods

Among the set of parameters of mathematical models of turbocharging systems, the symptoms of process diagnostics of the turbocharging system included such parameters of the main operational process as:

- rotational speed of the main power engine  $n_{ME}$ ;
- rotational speed of turbocharger rotor unit  $n_{TS}$ ;
- air temperature and pressure before  $t_1$ ,  $p_1$  and after the compressor  $t_2$ ,  $p_2$ ;
- temperature and pressure of exhaust gas before  $t_3$ ,  $p_3$  and after the turbine  $t_4$ ,  $p_4$ ; in relation to the fuel rail setting, and selected parameters of associated processes.

The lack of possibility to measure exhaust gas pressure before the turbine in turbochargers, which is necessary to determine the expansion of  $(p_4^*/p_3^*)$  the exhaust gas in the turbine, makes it impossible to determine the efficiency of the turbine in operation, according to relation (6). With the limited usefulness of the parametric diagnostic test for undertaking maintenance services on turbocharger systems, an attempt has been made to apply machine learning to turbocharger diagnosis.

## 5. Turbocharger diagnostics with the application of machine learning

The authors proposed a classification of the technical condition of a marine engine turbocharger based on the measurement signals of the main engine shaft speed and the charging air pressure at the compressor outlet. These parameters were selected basing on the analysis of available measurement signals of various turbocharged engines and the relationships between engine and turbocharger parameters. Figures 8 and 9 show clear correlations between the main engine shaft speed and the turbocharger rotor speed (Figure 9) and the charging air pressure and the turbocharger rotor speed (Figure 8). Based on these relationships, a strong dependence of charging air pressure on the main engine shaft speed was assumed.

It was found that a neural network with two input signals of the main engine speed  $n_{ME}$  and the charging air pressure  $p_2$  during machine learning would enable determination of the transformation function  $f_m$  of sets  $p_2$  and  $n_{ME}$  into a set of service necessity index  $M$

$$(p_2, n_{ME}) \xrightarrow{f_m} M \quad (7)$$

The relationship described by equation (7) was realized by the neural network shown in Figure 13. Multilayer neural networks taught by back propagation error are a classic method that is perfectly implemented in many utilities, including the Matlab *nnTool* tool.

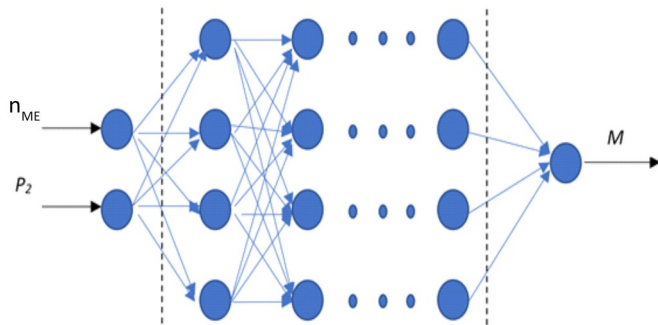


Fig. 13. A neural network implementing transformation (7)

## 6. Numeric experimental studies

For the proposed method of identifying the need for turbocharger overhaul, simulation has been carried out using the results of measurements based on the TCA55 turbocharger shown in Chapter 4, Figures 8-10. Figure 14 shows the dependence of the charging air pressure  $p_2$  on the main engine shaft speed  $n_{ME}$  at different engine loads.

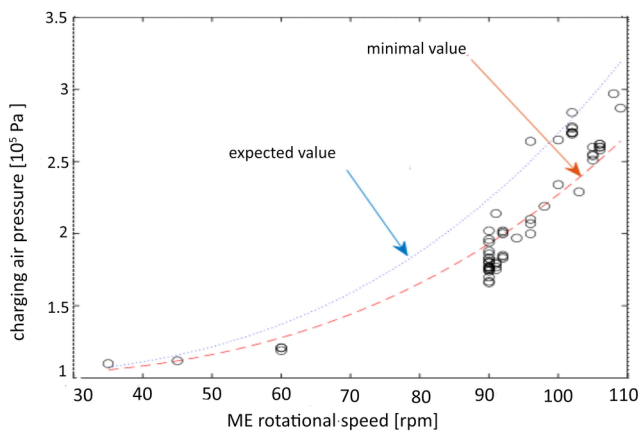


Fig. 14. A function describing the relationship between the expected values of air charge pressure  $p_{2ex}$  and a function describing the minimum acceptable values of air charge pressure  $p_{2min}$  in relation to the main engine shaft speed (ME)

In Figure 14, the blue curve indicates the expected value of air charging pressure  $p_{2ex}$  for the maximum turbocharger efficiency, determined by selecting maximum air charging pressure values for chosen main engine shaft speeds. The equation of the expected value curve  $p_{2ex}=f(n_{ME})$  was established as a trend line equation for these measurement points. The selected points and the equation of the trend line are shown in Figure 15.

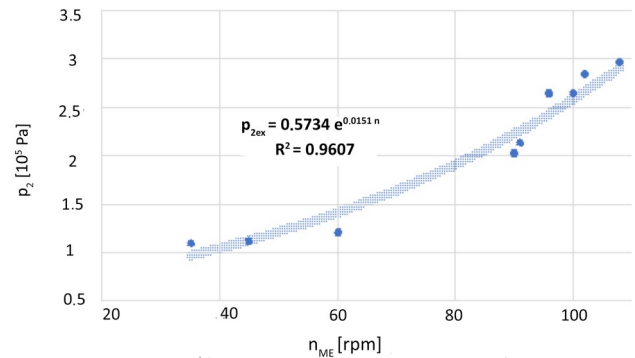


Fig. 15. Equation of the function of the expected values of charging air pressure

Figure 14 also shows in red the curve of the  $p_{2min}$  limit air charging values. The measurement results below the limiting values indicate the turbocharger is in a condition requiring service. For each measurement point the value of the index  $M$  has been assigned; for all points lying on the blue curve and above it, the need for servicing does not occur and the value of the coefficient is  $M = 0$ . For the points on the red line and below the curve the need for servicing occurs and the value of the index is  $M = 1$ . For the points situated between the lines the coefficient value was assumed to be linearly dependent on the measured value of the  $p_{2m}$  pressure

$$M = \frac{p_{2ex} - p_{2m}}{p_{2ex} - p_{2min}} \quad (8)$$

A plot of the variation of the  $M$ -value as a function of boost pressure and engine shaft speed is shown in Figure 16.

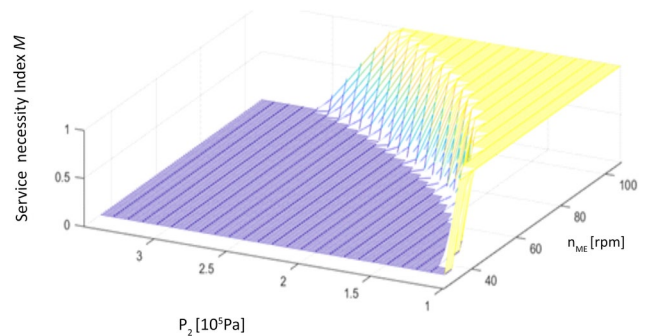


Fig. 16. Variability of the service necessity index  $M$

The machine learning experiment was carried out in MATLAB using the *nnTool* interface. Neural networks with one input signal can have a quite simple structure, e.g., for mapping the trigonometric function (sine or cosine), a simple 1-7-1 network with one hidden layer containing 7 neurons is enough. In the case of the described modelling of the  $M$  index depending on two input parameters, the neural network with one hidden layer did not bring positive results. During subsequent experiments, the network size was determined as 2-80-80-80-1 that is 4 layers hidden with 80 neurons in each layer. The

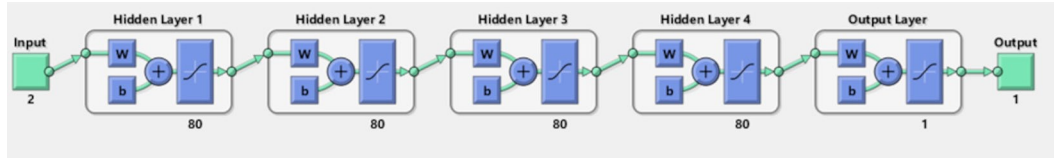


Fig. 17. Neural network structure

structure of the network is presented in Figure 17. In the hidden layers for all neurons, the *tansig* transfer function was used, which returns numerical values in the range  $\langle -1: 1 \rangle$ , while in the output layer the *logsig* function was used, which has the output value range  $\langle 0: 1 \rangle$ .

To network learning, a set of cases was generated containing 500 elements in the range of pressure and rotational speed values as shown in Figure 16. The values of the  $M$  index were determined according to equation (8). The data is shown in Figure 18. Case values are summarized in the form of a matrix

$$\begin{bmatrix} n_{ME} \\ p_2 \\ M \end{bmatrix} \quad (9)$$

with a size of  $3 \times 500$ . The first two lines containing the numerical values of the  $n_{ME}$  engine speed and the boost pressure  $p_2$  were the input values of the neural network (input), while the last line containing the values of the service necessity index  $M$  constituted the expected network responses (target). The set of cases was created in the following way: a set of 500 random values of the  $n_{ME}$  engine rotational speed in the value range  $\langle 35: 110 \rangle$  [rpm] was generated. Then the values of  $p_{2min}$  and  $p_{2ex}$  were determined for these values. Where  $p_{2ex}$  was calculated according to the equation presented in Figure 15. For the purposes of the experiment,  $p_{2min} = 0.75p_{2ex}$  was assumed. In the next step, 500 values of pressure  $p_{2m}$  were drawn from the interval  $\langle p_{2min}: p_{2ex} \rangle$ . With sets of  $n_{ME}$  and  $p_2$  values, the service necessity coefficient  $M$  was calculated according to equation (8). The numerical values of the  $M$  index used as the target set are in the range  $\langle 0: 1 \rangle$ , therefore the authors concluded that there is no need to normalize the data.

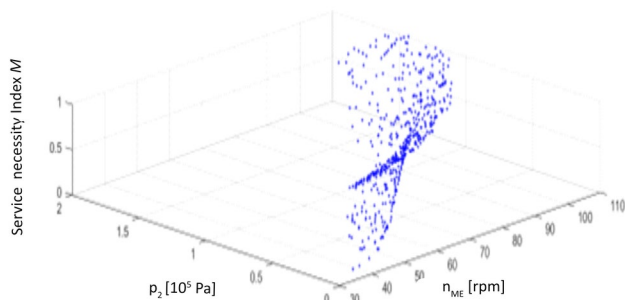


Fig. 18. Data for neural network learning

The *trainlm* function was selected to train the network, which implements non-linear Levenberg-Marquardt optimization. The *trainlm* function is often recommended as a supervised first choice algorithm. This function randomly divides the provided set of cases into the following subsets: *training set*, which is 1/2 of the case set, *validation set*, which is 1/4 of the case set, and *test set*, which is 1/4 a collection of cases. The validation set is used to evaluate the learning quality of the network and to decide whether to stop training early if the quality of the network's response to the validation vector (*max\_fail*) does not improve or remains the same for a specified number of consecutive epochs. The test set is used to monitor whether the network is generalizing correctly, but its results have no effect on the training progress.

The gradient descent with momentum weight and *bias* learning function was used to adapt the network, i.e., to change the weight value and the bias value. The function calculates the weight change for each neuron based on the input data, neuron error, weight or bias, learning rate coefficients and momentum.

The default parameters of the *trainlm* and *learn\_gdm* functions were used in the network learning:

$lp\_lr = 0.01$  learning rate,

$lp\_m = 0.9$  momentum,

$epochs = 1000$  - maximum number of epochs,

$goal = 0$  expected mapping error,

$max\_fail = 6$  validation error for a specified number of consecutive epochs,

$max\_fail\_epochs = 50$  number of epochs with invariant validation error

$min\_grad = 1e-7$  minimal performance gradient,

$mu = 0,001$  momentum change factor (initial value),

$mu\_dec = 0.1$  reduction factor of  $mu$ ,

$mu\_inc = 10$  growth factor of  $mu$ ,

$mu\_max = 1e10$  maximum value of  $mu$ ,

$time = inf$  maximum time of network training [s].

Figure 19 shows the process of learning the network with a division into the quality of mapping the training, validation, and test sets. Network training was completed after 211 iterations after the network mapping error condition was satisfied by subsequent generations (*max\_fail*). The best representation of the validation set, obtained in 161 iteration, was marked on the run. Over the next 50 epochs, the mapping error did not improve, which was the basis for completing network learning.

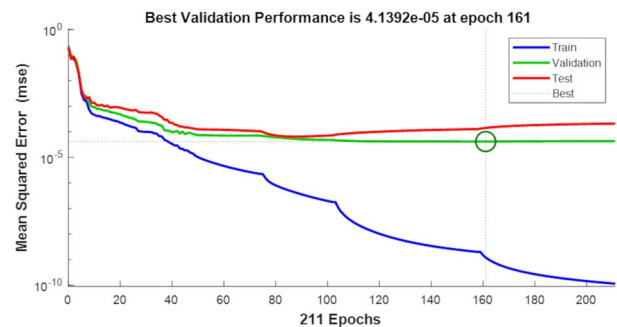


Fig. 19. The process of training a neural network

As a result of the network learning process, the correct mapping of the sets of boost pressure  $p_2$  and the rotational speed of the  $n_{ME}$  main engine into the service necessity index set was obtained. Figure 20 shows the results of linear regression R mapping individual sets by the neural network and their generalization.

After learning the neural network based on the generated set of cases, the correctness of the neural network response was verified using the real measurement data presented in Figure 14. The results of the measurements were returned by the neural network to the correct values of the maintenance necessity factor  $M$ . The obtained values of the index  $M$  were plotted on the course of the index variability (Fig. 16). The results are presented graphically in Figure 21.

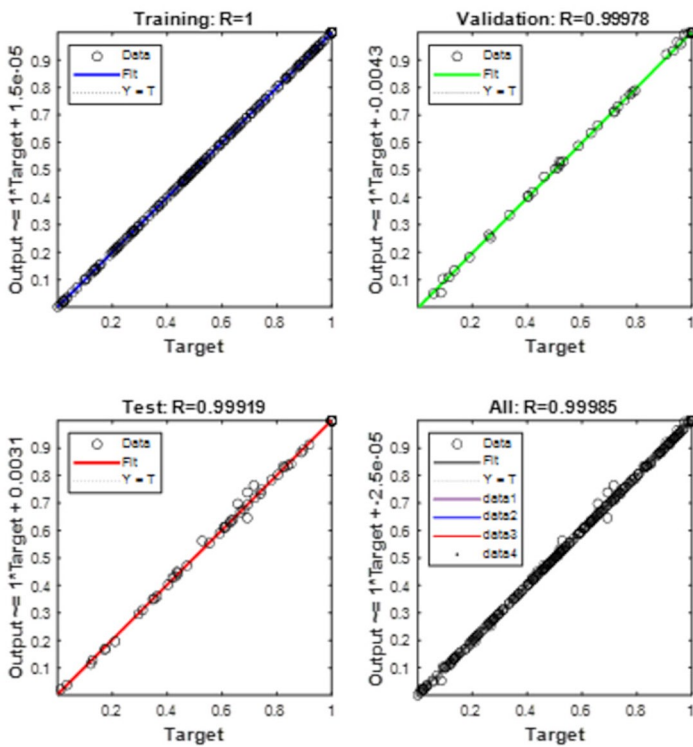


Fig. 20. The result from the neural network learning process in the form of linear regression

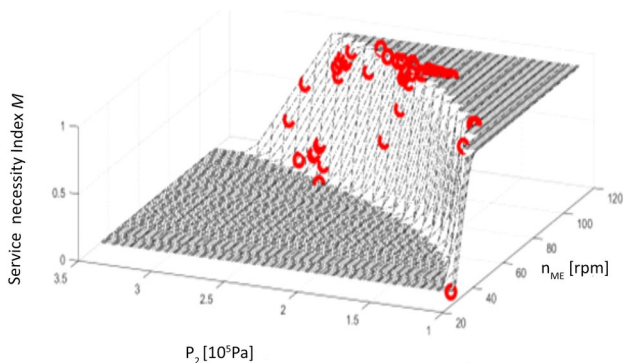


Fig. 21.  $M$  index values obtained from neural network for measurement points

## References

1. ABB Turbo Systems Ltd: Operational Manual TPL 77-A, 2007
2. Adamkiewicz A., Zeńczak W.: Diagnostyka systemu turbodoładowania okrętowego silnika o zapłonie samoczynnym podczas eksploatacji. DIAGO 2016 Technicka Diagnostika Asociace Technických Diagnostiku České Republiku, o.s., ISSN 1210-311X, Z1, ROČNIK XXV, Abstrakt book, CD 5-14
3. Anantharaman M., Khan F., Garaniya V., Lewarn B., Reliability Assessment of Main EGINE Subsystems Considering Turbocharger Failure as a Case Study. TransNav the International Journal on Marine Navigation and Safety of Sea Transportation 2018;12(2):271-276. Doi: 10.12716/1001.12.02.06
4. Anantharaman M, Islam R, Sardar A, Garaniya V, Khan F. Impact of defective turbocharging system on the safety and reliability of large marine diesel engine. TransNav : International Journal on Marine Navigation and Safety of Sea Transportation. 2021;15(1):189-198.
5. Burzyński K.: Analiza parametrów dopuszczalnych i granicznych stosowanych w diagnostyce cieplnych maszyn wirnikowych. Praca dyplomowa inżynierska, Akademia Morska w Szczecinie, Wydział Mechaniczny, Szczecin 2015.
6. Cui X, Yang C, Serrano JR, Shi M. A performance degradation evaluation method for a turbocharger in a diesel engine. R Soc Open Sci. 2018 Nov 14;5(11):181093. doi: 10.1098/rsos.181093. PMID: 30564402; PMCID: PMC6281929.
7. Deng, X. W., Gu, Y. J., Fang, L. P., Ren, Z. X., & Han, Y. P., Study of Intelligent Fault Diagnosis Method for Turbo-Generator Unit Based on Support Vector Machine and Knowledge. Applied Mechanics and Materials 2014; 543–547; 1057–1063. Trans Tech Publications, Ltd, <https://doi.org/10.4028/www.scientific.net/amm.543-547.1057>
8. Divya M.N, Modeling a Fault Detection Predictor in Compressor using Machine Learning Approach based on Acoustic Sensor Data,

## 7. Summary

Methods of control of operational parameters and supervision of turbocharging system functioning in marine engines, which are currently used, do not provide full information for making maintenance/service decisions, in accordance with the adopted operational strategy, classification society regulations and engine manufacturer's regulations. Current control and archiving systems of operational parameters of turbocharging systems may not always be expert systems with diagnostic reasoning. There are strong diagnostic relations between some of the operational parameters, resulting both from models of energy processes and from the obtained parametric diagnostic test results. They can be the basis for searching for methods of inference other than parametric ones. The experimentally found strong diagnostic relationships can be used to search for decisions based on other sources of information, such as machine learning. A turbocharger service necessity index  $M$  was proposed. Its values depended on the marine engine shaft speed  $n_{ME}$  and compressor outlet air pressure  $p_2$ . The process of teaching the artificial neural network the dependence of the indicator  $M = f(n_{ME}, p_2)$  was carried out. The neural network responses were verified using the data from measurements on a real marine engine and promising results were obtained. The simulation experiment conducted in this research demonstrated the usefulness of the proposed method in utilitarian diagnosis of turbochargers.

The authors conducted the first attempt to use artificial neural networks to classify a turbocharger for service work. Multilayer neural networks taught by back propagation error are a classic method. In the experiment, the authors focused on obtaining satisfactory results in the mapping of the proposed service necessity coefficient  $M$  based on the measured values of the engine speed  $n_{ME}$  and the boost pressure  $p_2$ . This is the first step of the authors in the use of neural networks for the service classification of a turbocharger. The next planned step is to extend the classification of the need for service to include the mechanical element of the turbocharger, i.e., turbine blades or compressor flow channels. These elements are shown in figures 1 and 2. After determining the measured parameters, based on which it is possible to indicate the place of maintenance of the turbocharger. The study of the problem during the research showed that there are other strong diagnostic relationships to be applied in decision support using artificial neural networks. One of them is the relationship of charge air pressure with turbocharger rotor unit speed and charge air pressure with fuel rail indicator [2]. This provides a basis for further experiments supporting turbocharger service decisions based on the values of these parameters. The authors plan experiments using methods other than error backpropagation.

- (IJACSA) International Journal of Advanced Computer Science and Applications 2021;12, (9); 650-667
9. Dong H., Zhao Z., Fu J., Liu J., Li J., Liang K., Zhou Q., Experiment and simulation investigation on energy management of a gasoline vehicle and hybrid turbocharger optimization based on equivalent consumption minimization strategy, *Energy Conversion and Management*, 2020; 226. [Doi.org/10.1016/j.enconman.2020.113518](https://doi.org/10.1016/j.enconman.2020.113518).
  10. Főző I., Andoga R., Madarász L., Kolesár J., Judičák J., Description of an intelligent small turbocompressor engine with variable exhaust nozzle, SAMI 2015, IEEE 13th International Symposium on Applied Machine Intelligence and Informatics, January 22-24, 2015, Herlany, Slovakia
  11. Guan C, Theotokatos G, Chen H. Analysis of Two Stroke Marine Diesel Engine Operation Including Turbocharger Cut-Out by Using a Zero-Dimensional Model. *Energies*. 2015; 8(6):5738-5764. <https://doi.org/10.3390/en8065738>
  12. Hipple S. M., Bonilla-Alvarado H., Pezzini P., Shadle L., Bryden K. M., Using Machine Learning Tools to Predict Compressor Stall, *Journal of Energy Resources Technology* 2020; 142; 072305-1- 072305-9
  13. Hountalas D.T.; Sakellariadis N.F.; Pariotis E.; Antonopoulos A.K.; Zissimatos L.; Papadakis N., Effect of turbocharger cut out on two-stroke marine diesel engine performance and NOx emissions at part load operation. In Proceedings of the ASME 12th biennial conference on engineering systems design and analysis, Copenhagen, Denmark, 25–27 July 2014. ESDA2014-20514
  14. Hriadel D. Health Status Monitoring of Turbocharger for Passenger Vehicle Applications, Master's Thesis, Czech Technical University in Prague, Department of Control Engineering, Prague, January 2019
  15. Knežević V., Orović J., Stazić L., Čulin J., Fault Tree Analysis and Failure Diagnosis of Marine Diesel Engine Turbocharger System, *Journal of Marine Science and Engineering* 2020; 8, (12), [doi:10.3390/jmse8121004](https://doi.org/10.3390/jmse8121004)
  16. Lau C., Maier M., Knowledge-based predictive maintenance for olefins turbocompressors, 2004 AIChE Spring National Meeting, Conference Proceedings; 611 – 625
  17. Liu C, Cao Y, Ding S, Zhang W, Cai Y, Lin A. Effects of blade surface roughness on compressor performance and tonal noise emission in a marine diesel engine turbocharger. Proceedings of the Institution of Mechanical Engineers, Part D: Journal of Automobile Engineering. 2020;234(14):3476-3490. [Doi:10.1177/0954407020927637](https://doi.org/10.1177/0954407020927637)
  18. Liu C., Cao Y., Liu Y.2, Zhang W., Ming P., Numerical investigation of marine diesel engine turbocharger compressor tonal noise. Proceedings of the Institution of Mechanical Engineers, Part D: Journal of Automobile Engineering. 2020;234 (1):71-84. [Doi: 10.1177/0954407019841808](https://doi.org/10.1177/0954407019841808)
  19. MAN B&W Turbocharger. Cleaning the Turbine – Benefits of Dry Cleaning at operating load. Diesel Customer Information. MAN B&W Diesel AG 86224 Augsburg Cus 228, 06/06
  20. Medica, V., Račić, N., & Radica, G. (2009). Performance simulation of marine slow-speed diesel propulsion engine with turbocharger under aggravated conditions. *Strojtarstvo*, 51(3), 199-212
  21. Nguyen-Schafer, H. Rotodynamics of Automotive Turbochargers. Springer. 2015,XV, 362 p. 222. Chapter 2 Thermodynamics of Turbochargers. ISBN: 978-3-3-319-17643-7.
  22. Nnaji, O.E., Nkoi, B., Lilly, M.T., Le-ol, A.K.: Evaluating the Reliability of a Marine Diesel Engine Using the Weibull Distribution. *Journal of Newviews in Engineering and Technology (JNET)*. 2, 2, 1–9 (2020).
  23. Pawełczyk M, Fulara S, Sepe M, De Luca A, Badora M. Industrial gas turbine operating parameters monitoring and data-driven prediction. *Eksploracja i Niezawodność – Maintenance and Reliability* 2020; 22 (3): 391–399, <http://dx.doi.org/10.17531/ein.2020.3.2>
  24. Prytz, Rune et al. (2015). “Predicting the need for vehicle compressor repairs using maintenance records and logged vehicle data.” In: *Engineering applications of artificial intelligence* 2015;41: 139–150. [Doi: 10.1016/j.engappai.2015.02.009](https://doi.org/10.1016/j.engappai.2015.02.009)
  25. Tabaszewski M, Szymański G. M. Engine valve clearance diagnostics based on vibration signals and machine learning methods. *Eksploracja i Niezawodność – Maintenance and Reliability* 2020; 22 (2): 331–339, <http://dx.doi.org/10.17531/ein.2020.2.16>.
  26. Taylor J.V, Conduit B., Dickens A., Hall C., Hillel M., Miller R. J., Predicting the Operability of Damaged Compressors Using Machine Learning, *Journal of Turbomachinery* 2020; 142; 051010-1: 051010-8, DOI: 10.1115/1.4046458,
  27. Turbocharging Efficiencies - Definitions and Guidelines for Measurement and Calculation. International Council on Combustion Engines. CIMAC Working Group “Turbocharger Efficiency“ and approved by CIMAC in May 2007, Frankfurt, Germany, Number 27/2007
  28. Vanhaelst, R., Kheir, A., Czajka, J., A systematic analysis of the friction losses on bearings of modern turbocharger. *Combustion Engines*,2015; 55(1), 22-31
  29. Varbanets R., Fomin, O., Pištěk V., Klymenko V., Minchev D., Khrulev A., Kučera P., Acoustic method for estimation of marine low-speed engine turbocharger parameters. *Journal of Marine Science and Engineering*, 2021;9(3), 321.
  30. Vrettakos NA. Analysis and characterization of a marine turbocharger’s unstable performance. Proceedings of the Institution of Mechanical Engineers, Part M: Journal of Engineering for the Maritime Environment. 2018;232(3):293-306. [doi:10.1177/1475090217693118](https://doi.org/10.1177/1475090217693118)
  31. Witkowski K.: Research on Influence of Condition Elements the Supercharger System On The Parameters Of The Marine Diesel Engine *Journal of KONES Powertrain and Transport*, Vol. 20, No. 1 2013
  32. Yi W., Hailong L., Gengxuan C., Jiawei Y., Fault Diagnosis of Marine Turbocharger System Based on an Unsupervised Algorithm, *Journal of Electrical Engineering & Technology* DA - 2020; 05(01), <https://doi.org/10.1007/s42835-020-00375-z>
  33. Zhang, J., Sun, H., Hu, L., and He, H., Fault diagnosis and failure prediction by thrust load analysis for a turbocharger thrust bearing. In *Turbo Expo: Power for Land, Sea, and Air*. 2010;44014: 491-498